

Superstructure-dependent electronic states in CaAlSi superconductors studied by angle-resolved photoemission spectroscopy

T. Sato,¹ Y. X. Xiao,¹ S. Souma,² K. Nakayama,¹ K. Sugawara,² S. Kuroiwa,³ J. Akimitsu,³ and T. Takahashi^{1,2}

¹*Department of Physics, Tohoku University, Sendai 980-8578, Japan*

²*WPI Research Center, Advanced Institute for Materials Research, Tohoku University, Sendai 980-8577, Japan*

³*Department of Physics and Mathematics, Aoyama-Gakuin University, Sagamihara, Kanagawa 229-8558, Japan*

(Received 18 February 2015; revised manuscript received 22 April 2015; published 11 May 2015)

We have performed high-resolution angle-resolved photoemission spectroscopy on layered polymorph series of $1H$ -, $5H$ -, and $6H$ -CaAlSi, which exhibit superconductivity below 6.5, 5.7, and 7.7 K, respectively. While the overall band structure in the valence-band region is similar among these compounds, the volume of the Fermi surface at the M point and the magnitude of the superconducting gap are markedly different from each other. Implications of such variation in the electronic structure due to the superstructure along the c axis are discussed in relation to the physical properties of CaAlSi.

DOI: [10.1103/PhysRevB.91.195114](https://doi.org/10.1103/PhysRevB.91.195114)

PACS number(s): 74.70.Ad, 74.25.Jb, 79.60.Bm, 71.20.-b

I. INTRODUCTION

Since the discovery of superconductivity in MgB₂ with a transition temperature T_c of 39.7 K [1], intermetallic compounds with a simple AlB₂-type structure have attracted much attention. Among various AlB₂-type compounds, ternary silicides M AlSi and M GaSi ($M = \text{Ca, Sr, Ba}$) have been the target of intensive studies since most of these compounds show superconductivity [2–9], with the highest T_c of ~ 8 K in CaAlSi [2]. As shown in Fig. 1, CaAlSi with $1H$ structure ($1H$ -CaAlSi) is composed of alternately stacked Ca and Al/Si layers, where the Al/Si atoms are distributed regularly in the honeycomb B₂ plane [10]. It has been reported by synchrotron x-ray and neutron diffraction analyses that CaAlSi exhibits the superstructure along the c axis owing to the buckling and/or rotation of the AlSi layer [11] where the $5H$ ($6H$) compound has a c -axis length of five (six) times longer than that of its undistorted $1H$ counterpart [10]. Intriguingly, physical properties of these compounds were turned out to be different from each other. For instance, magnetic-susceptibility measurement indicated different T_c values of 6.5, 5.7, and 7.7 K for the $1H$ -, $5H$ -, and $6H$ samples, respectively [10,12]. Specific-heat measurement also suggested that the characteristics of superconductivity ranges from the weak-coupling ($1H$ case) to the strong-coupling ($6H$ case) regime [10]. The *ab initio* band-structure calculation predicted a strong reconstruction of electronic states owing to the backfolding of bands along the c^* axis due to the superstructure formation [13]. These results indicate that CaAlSi polymorphs provide a precious opportunity for investigating the relationship among crystal structure, superconducting properties, and electronic states.

An early angle-resolved photoemission spectroscopy (ARPES) study of CaAlSi (note that the sample likely includes various different polymorphs) has revealed two different Fermi-surface sheets each centered at the Γ and M points in the hexagonal Brillouin zone [14], which arise from the interlayer states of the Ca $3d$ orbital [15,16] hybridized with the Al/Si sp states. The superconducting gaps on different Fermi surfaces were found to be nearly of the same magnitude, suggesting the Fermi-surface-independent isotropic s -wave pairing symmetry [14] in contrast to the two-gap

superconductivity in MgB₂ [17,18]. However, it is still unresolved why the superconducting temperature is different for different polymorphs and how the superstructure is related to the electronic structure and, as a result, to the superconductivity.

In this paper, we report high-resolution ARPES studies of various CaAlSi polymorphs and demonstrate the distinct difference in the normal-state band structure and the superconducting-gap properties among $1H$ -, $5H$ -, and $6H$ -CaAlSi. In particular, we found that the volume of the electronlike Fermi surface at the M point and the superconducting-gap magnitude are distinctly different among different polymorphs. The present result unambiguously demonstrates a close relationship between the superconducting properties and the superstructure-induced changes in the electronic states in CaAlSi polymorphs.

II. EXPERIMENT

Single crystals of $1H$ -, $5H$ -, and $6H$ -CaAlSi were grown using the floating-zone method [10]. X-ray diffraction measurements indicated the single-domain nature without inclusion from different polymorphs for each samples. We have estimated the T_c value using the magnetic susceptibility measurement to be 6.5, 5.7, and 7.7 K for $1H$ -, $5H$ -, and $6H$ -CaAlSi, respectively. A CaAlSi crystal cleaves between the AlSi and Ca layers, and the topmost surface layer is either the AlSi or Ca layer. Because of the large spot size ($\sim 2 \times 2$ mm) of incident light, the obtained ARPES data would reflect the electronic states for these two surface terminations. High-resolution ARPES measurements were performed using a VG-Scienta SES2002 spectrometer with a helium-plasma-discharge lamp and a toroidal grating monochromator. We used the He I α resonance line ($h\nu = 21.218$ eV) to excite photoelectrons. The energy resolution was set at 1.8–5.9 meV. We cleaved the samples *in situ* in a working vacuum better than 5×10^{-11} Torr to obtain a clean surface. The temperature of the sample was monitored by a silicon diode sensor embedded near the sample substrate, and its accuracy and stability during the measurement were less than 0.2 K. The Fermi level E_F of samples was referenced to that of a gold film evaporated onto the sample substrate.

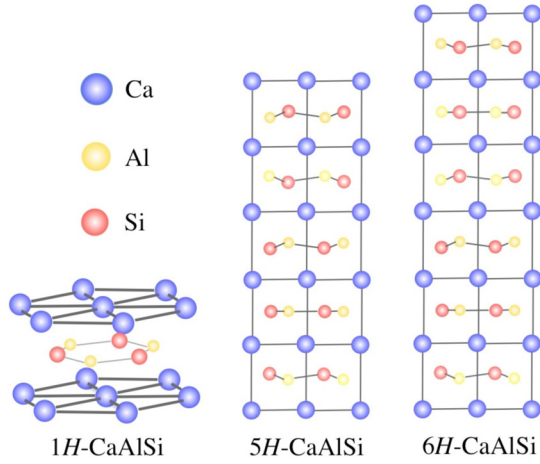


FIG. 1. (Color online) Crystal structures of 1H-, 5H-, and 6H-CaAlSi. The superconducting transition temperature is 6.5, 5.7, and 7.7 K, respectively.

III. RESULTS

Figures 2(a) and 2(b) show ARPES spectra of superstructure-free 1H-CaAlSi ($T_c = 6.5$ K) measured at $T = 20$ K with the He I α line ($h\nu = 21.218$ eV) along the ΓM and ΓKM high-symmetry cuts, respectively. We find highly dispersive bands in both cuts, indicative of the good surface quality of the sample. Two electronlike bands centered at the Γ point with their bottoms at ~ 1 and ~ 2 eV are clearly resolved in both cuts. As seen in Fig. 2(a), several peaks are observed around the M point. A band located near E_F clearly crosses E_F , forming an electron pocket at the M point, consistent with the previous ARPES report [14] [note that the ARPES spectra around the M point along the ΓKM cut in Fig. 2(b) are relatively featureless compared to that along the ΓM cut in Fig. 2(a), likely due to the difference in the light polarization with respect to the crystal axis, as indicated in the insets in Figs. 2(a) and 2(b)].

To see more clearly the dispersive feature of bands, we have mapped out the band structure and show the result in Figs. 2(c) and 2(d). The experimental band structure was obtained by taking the second derivative of ARPES spectra and plotting the intensity by gradual shading as a function of wave vector and binding energy. The band structure calculations [16] for 1H-CaAlSi along the ΓM (AL) and ΓKM (AHL) lines in the bulk Brillouin zone are superimposed on the experimental results. Comparison between the experiment and the calculation suggests that the electronlike band centered at the Γ (A) point with the band bottom at 2 eV is assigned as the Al/Si $3p\pi$ band. On the other hand, the electronlike band at the Γ (A) point with the bottom at 1 eV in the experiment has no counterpart in the calculation, suggesting that it is of surface-state origin [14]. The theoretical holelike σ bands at the Γ (A) point are not clearly resolved in the ARPES experiment, probably due to the photoelectron matrix-element effect [14]. The interlayer (IL) band which forms a three-dimensional (3D) electron pocket at the Γ point in the calculation may be pushed upward into the unoccupied region in the experiment. A shallow electron pocket observed at the M (L) point in the experiment [Fig. 2(c)] would correspond to the interlayer band

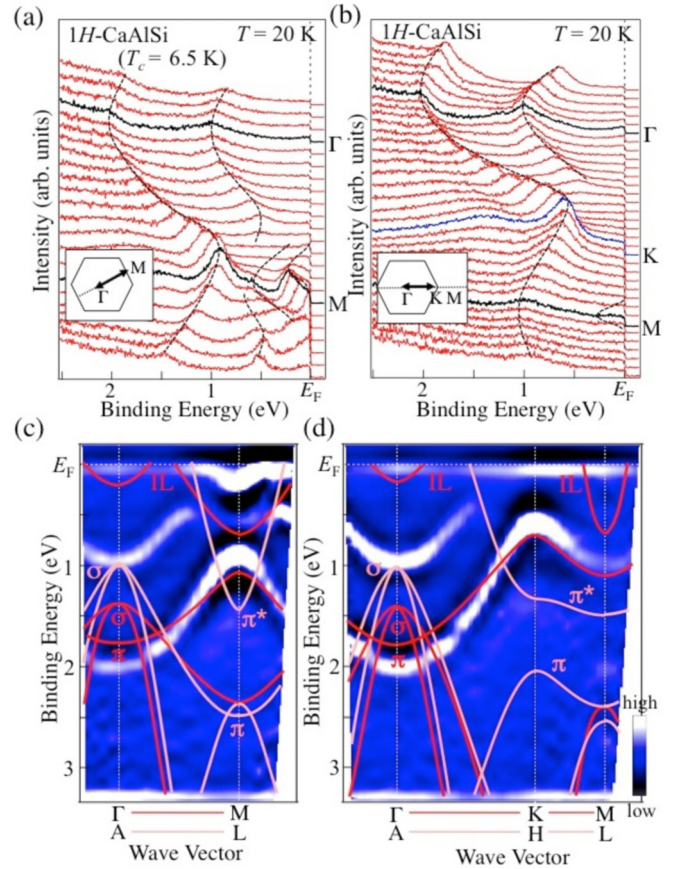


FIG. 2. (Color online) (a) and (b) ARPES spectra of 1H-CaAlSi along the ΓM and ΓKM cuts, respectively, measured at $T = 20$ K with the He I α line ($h\nu = 21.218$ eV). Dashed curves are a guide for the eyes to trace the band dispersion. The inset shows the polarization vector of incident light (arrow) in the surface Brillouin zone. (c) and (d) Second-derivative intensity of ARPES spectra as a function of wave vector and binding energy for ΓM and ΓKM cuts. Red (pink) curves are the calculated band dispersions [16] for ΓM and ΓKM (AL and AHL) lines.

(which hybridizes with the π band), forming a 3D electron pocket at the M point, while the experimental band dispersion appears to be much shallower than the calculated band, likely due to a finite k_z dispersion of the interlayer band and/or band-mass renormalization induced by electron correlation. The observation of a large electron pocket is also consistent with the Seebeck coefficient, which indicated majority charge carriers of electrons in contrast to the holes in MgB_2 [5].

Next, we show the superstructure dependence of the valence-band structure. Figure 3 displays the ARPES spectra and the corresponding experimental band dispersions along the ΓKM cut for 1H-, 5H-, and 6H-CaAlSi. One can immediately recognize a similarity in the overall feature of band dispersions. In particular, the electronlike π band and the surface states at the Γ point are commonly observed in all the compounds. A careful look at Figs. 3(d)–3(f) reveals that the bottom of the surface band at the Γ point is slightly (by 0.1 eV) higher in 1H-CaAlSi than those in 5H- and 6H-CaAlSi. In addition, the top of the bulk electronlike π band at the K point is slightly (by 0.2 eV) lower in 5H-CaAlSi than those in 1H- and 6H-CaAlSi. The observed small variation

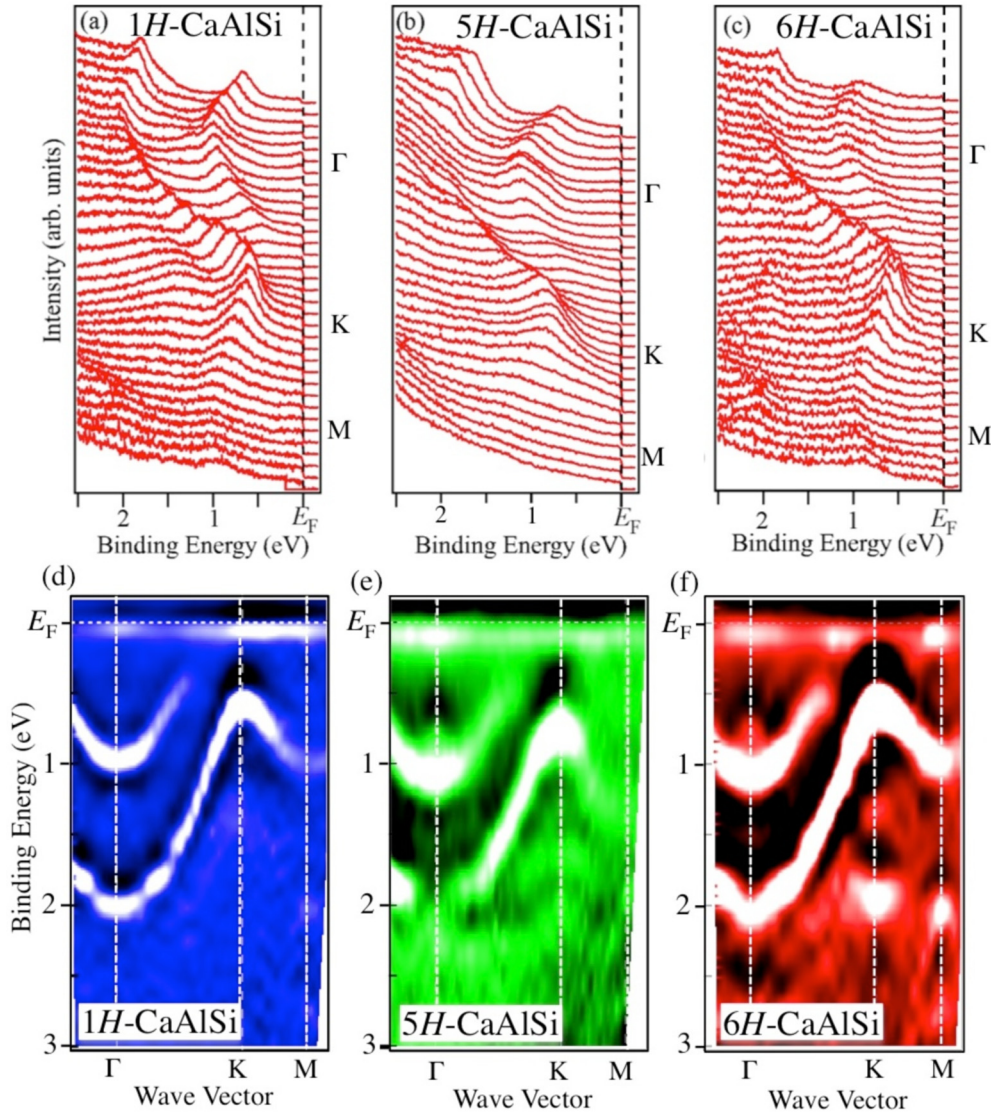


FIG. 3. (Color online) (a)–(c) ARPES spectra and (d)–(f) corresponding experimental band dispersions along the $\Gamma K M$ cut for 1H-, 5H-, and 6H-CaAlSi.

in the overall valence-band feature suggests that the periodic potential due to the c -axis superstructure is not as strong as that expected from the band-structure calculation [13], which has predicted the complicated band structure and the resultant multiple Fermi-surface sheets due to the band folding along the c^* axis. We speculate that the broader spectral feature of 5H- and 6H-CaAlSi compared to that of 1H-CaAlSi in Figs. 3(a)–3(c) is likely a reflection of the weak periodic potential since it can be explained by the emergence of weak multiple subbands (around the main band) created by the band folding.

In contrast to the observed small variation in the valence-band structure, the near- E_F band dispersion exhibits a strong superstructure dependence. Figures 4(a)–4(c) show the ARPES spectra near E_F measured along the ΓM cut for three different polymorphs with the same photon energy ($h\nu = 21.218$ eV). Taking into account the weak superstructure potential, it would be possible to regard the length between two adjacent Ca planes (which is identical to the c -axis length of 1H-CaAlSi) as an “effective” c -axis length for the sake of

direct comparison of lattice parameters. According to previous studies [10,11,13], the variation of this effective c -axis length is very small (less than 1%) in 1H-, 5H-, and 6H-CaAlSi. We thus conclude that the scanned plane in the three-dimensional momentum space is essentially similar in these samples. As shown in Figs. 4(a)–4(c), we immediately find that the band dispersion around the M point is markedly different for different polymorphs. This is better illustrated by a direct comparison of ARPES spectrum at the M point in Fig. 4(d), where we find that the peak closest to E_F (indicated by an arrow) is located at ~ 0.25 , ~ 0 , and ~ 0.1 eV for 1H-, 5H-, and 6H-CaAlSi, respectively. This variation in the energy position of the electronlike band is reflected in the plot of ARPES intensity at E_F in Fig. 4(e), which displays the largest (smallest) Fermi surface in 1H-CaAlSi (5H-CaAlSi). We will come back to this point later. The reason why the electronlike band near E_F at the M point shows a stronger superstructure dependence than the other valence-band feature is unclear at present. One possible explanation is the difference in the

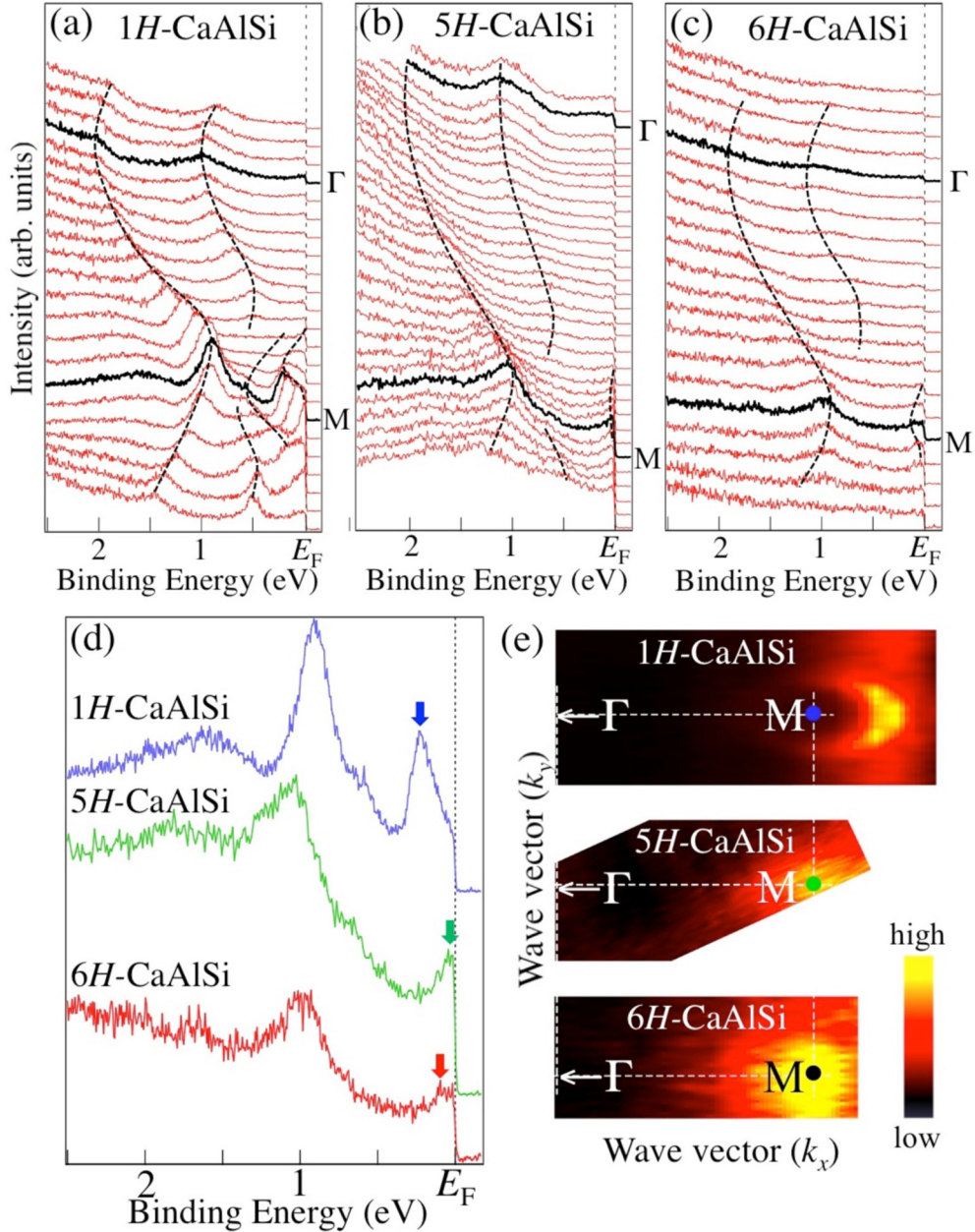


FIG. 4. (Color online) (a)–(c) ARPES spectra along the ΓM cut for 1H-, 5H-, and 6H-CaAlSi, respectively. Dashed curves are a guide for the eyes to trace the band dispersion. ARPES spectra at the Γ and M points are indicated by black curves. (d) Comparison of the ARPES spectrum at the M point among 1H-, 5H-, and 6H-CaAlSi. Arrows indicate the energy position of the near- E_F band. (e) ARPES intensity at E_F as a function of in-plane wave vector (k_x and k_y).

orbital character of the bands. Namely, the electron pocket which originates from the mixture of the interlayer and π orbitals has an electronic wave function more extended toward the c -axis direction compared to the σ band. This situation may favor of a stronger band modulation by the c -axis periodic potential.

Having established the near- E_F electronic states around the M point, the next important question is whether the superconducting-gap magnitude is different among these three polymorphs. To address this question, we have performed ultrahigh-resolution ARPES measurements at a selected k point along the MK cut on the electronlike Fermi surface.

Figure 5 shows the ultrahigh-resolution ARPES spectra near E_F for 1H-, 5H-, and 6H-CaAlSi measured at temperatures above and below the superconducting transition temperature. In the spectra at 4.3 K, we clearly find a pileup of spectral weight at 2–4 meV below E_F , which shows the emergence of a superconducting quasiparticle peak. Simultaneously, the midpoint of the leading edge in the spectrum shifts toward higher binding energy, accompanied by a reduction in the spectral weight at E_F . This clearly demonstrates an opening of the superconducting gap. In sharp contrast, the ARPES spectrum at $T = 10.5$ K appears to show no well-defined peak or leading-edge shift, reflecting the absence of an energy gap. We have

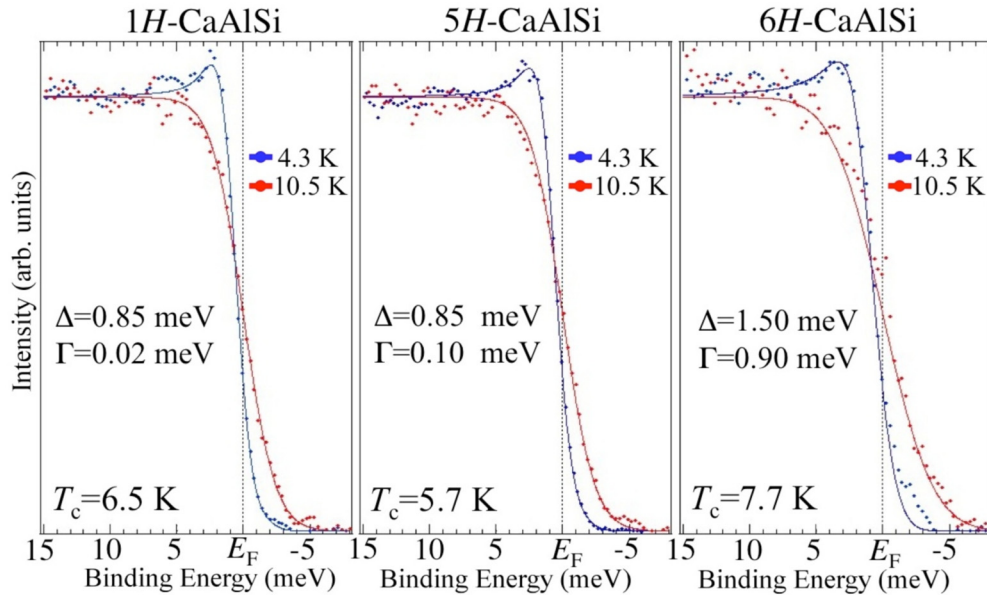


FIG. 5. (Color online) Ultrahigh-resolution ARPES spectra measured at $T = 4.3$ K (superconducting state) and 10.5 K (normal state) for $1H$ -, $5H$ -, and $6H$ -CaAlSi. Blue and red solid curves are the numerical fittings with the Dynes function [19] (superconducting state) and the Fermi-Dirac function (normal state), respectively. Obtained fitting-parameter values of the Dynes function for the superconducting gap Δ and the broadening factor Γ are also indicated.

numerically fitted the ARPES spectra at $T = 4.3$ K with the Dynes function [19] multiplied by the Fermi-Dirac distribution function convoluted with a Gaussian representing the energy resolution (FWHM of 1.8 meV), and we have found the gap value Δ to be 0.85 , 0.85 , and 1.50 meV for $1H$ -, $5H$ -, and $6H$ -CaAlSi, respectively. This indicates that the superstructure substantially influences the superconducting gap in CaAlSi.

IV. DISCUSSION

Now we discuss the implications of the present ARPES results in relation to other experiments. The difference in the Fermi-surface volume [Figs. 4(d) and 4(e)] suggests that the density of states (DOS) at E_F is the highest in $1H$ -CaAlSi, while it is the lowest in $5H$ -CaAlSi. Interestingly, a similar trend is also seen in the electronic specific-heat coefficient γ_m of 6.10 , 3.86 , and 5.07 mJ mol $^{-1}$ K $^{-2}$ for $1H$ -, $5H$ -, and $6H$ -CaAlSi, respectively [10]. Taking into account that γ_m reflects the k -averaged quasiparticle DOS, it is inferred that the electron pocket at the M point has a dominant contribution to the quasiparticle DOS. It is also noted that the superconducting-gap magnitude estimated by the ARPES and the specific-heat measurements show good agreement with each other. The ARPES gap magnitude derived by assuming mean-field-like temperature dependence is $2\Delta(0)/k_B T_c = 3.6$, 4.7 , and 5.0 for $1H$ -, $5H$ -, and $6H$ -CaAlSi, respectively, where $\Delta(0)$ represents the superconducting-gap size at $T = 0$ K. On the other hand, the gap magnitude estimated from the specific heat [10] is ~ 3.5 , 4.41 , and 5.25 , showing good agreement with the ARPES results. This indicates that the superconducting gap observed by ARPES is of bulk origin, and the superstructure formation converts the originally weak-coupling superconductivity in $1H$ -CaAlSi into the strong-

coupling superconductivity in $5H$ - and $6H$ -CaAlSi, possibly due to the change in the electronic structure.

Finally, we discuss the physical mechanism behind the T_c variation upon introducing superstructure. The structural distortion in the conducting Al/Si plane is expected to reduce T_c , as inferred from the investigation of CaSi $_2$ [20,21], where application of pressure causes a structural transition toward the AlB $_2$ -like phase with higher T_c . In this context, the highest T_c would be realized in $1H$ -CaAlSi, where the conducting Al/Si layer has no structural distortion, and lower T_c values are expected for $5H$ - and $6H$ -CaAlSi, which contain buckled/rotated Al/Si layers. However, while this argument succeeds in explaining the lower T_c value in $5H$ -CaAlSi (5.7 K) than in $1H$ -CaAlSi (6.5 K), the observed highest T_c (7.7 K) in $6H$ -CaAlSi is hardly reconciled, indicating a different mechanism dominates T_c . For the BCS-type superconducting pairing mediated by the electron-phonon coupling, the DOS at E_F is a key ingredient for determining T_c (assuming that the phonon DOS is fixed). The higher T_c in $1H$ -CaAlSi (or $6H$ -CaAlSi) than in $5H$ -CaAlSi may be a consequence of this effect, although the highest T_c in $6H$ -CaAlSi is still hardly explained even with this scenario. It is thus inferred that the change in the electron-phonon-coupling strength (i.e., the phonon DOS), presumably assisted by the change in the dimensionality, needs to be taken into account to understand the unconventional T_c variation upon superstructure formation.

V. SUMMARY

We have reported high-resolution ARPES results for $1H$ -, $5H$ -, and $6H$ -CaAlSi. We have revealed that the volume of the Fermi surface at the M point and the magnitude of the superconducting gap are markedly different among the three polymorphs, providing direct experimental evidence for

the superstructure-induced modification of electronic states and superconducting properties. Comparison of the ARPES results with the specific-heat experiment suggests an important contribution of electronic states at the M point to the superconductivity.

ACKNOWLEDGMENT

This work was supported by grants from the Japan Society for the Promotion of Science (Grants No. KAKENHI 23224010 and No. 25287079).

-
- [1] J. Nagamatsu, N. Nakagawa, T. Muranaka, Y. Zenitani, and J. Akimitsu, *Nature (London)* **410**, 63 (2001).
 - [2] M. Imai, K. Nishida, T. Kimura, and H. Abe, *Appl. Phys. Lett.* **80**, 1019 (2002).
 - [3] M. Imai, K. Nishida, T. Kimura, H. Kitazawa, H. Abe, H. Kito, and K. Yoshii, *Phys. C (Amsterdam, Neth.)* **382**, 361 (2002).
 - [4] M. Imai, E.-H. S. Sadki, H. Abe, K. Nishida, T. Kimura, T. Sato, K. Hirata, and H. Kitazawa, *Phys. Rev. B* **68**, 064512 (2003).
 - [5] B. Lorenz, J. Lenzi, J. Cmaidalka, R. L. Meng, Y. Y. Sun, Y. Y. Xue, and C. W. Chu, *Phys. C (Amsterdam, Neth.)* **383**, 191 (2002).
 - [6] B. Lorenz, J. Cmaidalka, R. L. Meng, and C. W. Chu, *Phys. Rev. B* **68**, 014512 (2003).
 - [7] T. Nakagawa, M. Tokunaga, and T. Tamegai, *Sci. Technol. Adv. Mater.* **7**, S108 (2006).
 - [8] S. Yamanaka, T. Otsuki, T. Ide, H. Fukuoka, R. Kumashiro, T. Rachi, K. Tanigaki, F.-Z. Guo, and K. Kobayashi, *Phys. C (Amsterdam, Neth.)* **451**, 19 (2007).
 - [9] M. J. Evans, Y. Wu, V. F. Kranak, N. Newman, A. Reller, F. J. Garcia-Garcia, and U. Häussermann, *Phys. Rev. B* **80**, 064514 (2009).
 - [10] S. Kuroiwa, H. Sagayama, T. Kakiuchi, H. Sawa, Y. Noda, and J. Akimitsu, *Phys. Rev. B* **74**, 014517 (2006).
 - [11] H. Sagayama, Y. Wakabayashi, H. Sawa, T. Kamiyama, A. Hoshikawa, S. Harjo, K. Uozato, A. K. Ghosh, M. Tokunaga, and T. Tamegai, *J. Phys. Soc. Jpn.* **75**, 043713 (2006).
 - [12] L. Boeri, J. S. Kim, M. Giantomassi, F. S. Razavi, S. Kuroiwa, J. Akimitsu, and R. K. Kremer, *Phys. Rev. B* **77**, 144502 (2008).
 - [13] S. Kuroiwa, A. Nakashima, S. Miyahara, N. Furukawa, and J. Akimitsu, *J. Phys. Soc. Jpn.* **76**, 113705 (2007).
 - [14] S. Tsuda, T. Yokoya, S. Shin, M. Imai, and I. Hase, *Phys. Rev. B* **69**, 100506(R) (2004).
 - [15] I. I. Mazin and D. A. Papaconstantopoulos, *Phys. Rev. B* **69**, 180512(R) (2004).
 - [16] M. Giantomassi, L. Boeri, and G. B. Bachelet, *Phys. Rev. B* **72**, 224512 (2005).
 - [17] S. Souma, Y. Machida, T. Sato, T. Takahashi, H. Matsui, S.-C. Wang, H. Ding, A. Kaminski, J. C. Campuzano, S. Sasaki, and K. Kadowaki, *Nature (London)* **423**, 65 (2003).
 - [18] S. Tsuda, T. Yokoya, Y. Takano, H. Kito, A. Matsushita, F. Yin, J. Itoh, H. Harima, and S. Shin, *Phys. Rev. Lett.* **91**, 127001 (2003).
 - [19] R. C. Dynes, V. Narayanamurti, and J. P. Garno, *Phys. Rev. Lett.* **41**, 1509 (1978).
 - [20] P. Bordet, M. Affronte, S. Sanfilippo, M. Núñez-Regueiro, O. Laborde, G. L. Olcese, A. Palenzona, S. LeFloch, D. Levi, and M. Hanfland, *Phys. Rev. B* **62**, 11392 (2000).
 - [21] S. Sanfilippo, H. Elsinger, M. Núñez-Regueiro, O. Laborde, S. LeFloch, M. Affronte, G. L. Olcese, and A. Palenzona, *Phys. Rev. B* **61**, R3800 (2000).